7818 *Inorg. Chem.* **2010**, *49*, 7818–7825
DOI: 10.1021/ic100851b

Inorganic Chemistry
Article

Bright Sky-Blue Phosphorescence of [*n*-Bu_4N][Pt(4,6-dFppy)$(CN)_2$]: Synthesis, Crystal Structure, and Detailed Photophysical Studies

Andreas F. Rausch,[†] Uwe V. Monkowius,*[,‡] Manfred Zabel,[§] and Hartmut Yersin*[,†]

[†]*Institut für Physikalische und Theoretische Chemie, Universität Regensburg, 93053 Regensburg, Germany,*
[‡]*Institut für Anorganische Chemie, Johannes Kepler Universität Linz, 4040 Linz, Austria, and*
[§]*Zentrale Analytik der Universität Regensburg, Röntgenstrukturanalyse, 93053 Regensburg, Germany*

Received April 29, 2010

This work describes the synthesis, crystal structure, and detailed photophysical studies of [*n*-Bu_4N][Pt(4,6-dFppy)-$(CN)_2$] (*n*-Bu = *n*-butyl, 4,6-dFppy = (4′,6′-difluorophenyl)pyridinate). The material can easily be prepared in high yield and purity by the reaction of [Pt(4,6-dFppy)(H-4,6-dFppy)Cl], [*n*-Bu_4N]Cl, and KCN in CH_2Cl_2. Because of the bulky counterion [*n*-Bu_4N]$^+$, Pt−Pt interactions, which frequently lead to aggregate formation, are suppressed in the solid state. Thus, monomer emission is observed. The phosphorescence quantum yield of the neat powder amounts to ϕ_{PL} = 60% at ambient temperature and decays with 19 μs. In tetrahydrofuran (THF) solution, on the other hand, the emission decay time is with 0.26 μs distinctly shorter, and the quantum yield is very low. By means of emission decay time studies in frozen THF and investigations of the highly resolved single crystal emission at 1.2 K, we can assign the emitting T_1 state of the compound as being largely of ligand centered (^{3}LC, $^3\pi\pi^*$) character. The observed differences of the emission properties of the neat powder compared to the fluid solution are rationalized with an energy stabilization of quenching dd* states in solution because of molecular distortions and/or bond elongations.

1. Introduction

Phosphorescent organo-transition metal compounds have stepped into the focus of scientific and industrial interest because of their applicability as efficient emitters in organic light emitting diodes (OLEDs),[1−6] light-emitting electrochemical cells (LECs),[7−9] and solid-state electroluminescent devices.[10−12] As a consequence of spin−orbit coupling (SOC) induced by the heavy metal center, devices incorporating such triplet emitting materials allow both singlet and triplet excitons to be utilized for the emission in an electroluminescence process, leading to a principally four times higher internal electroluminescence quantum yield than achievable with fluorescent emitters according to the triplet harvesting effect.[13−15] Further, a strong increase of the radiative decay rate and thus of the efficiency at high brightness applications is possible by the implementation of emitters which utilize the recently proposed singlet harvesting effect.[16]

Up to now, many efficient green- and red-emitting compounds have been reported. On the other hand, complexes exhibiting a blue emission of high quantum yield are rare, since non-radiative deactivation via thermally populated metal centered dd* states becomes an important problem with increasing emission energy.[17−19] Strategies to avoid the thermal population of such states by pushing them out of reach at ambient temperature make use, for example, of chromophoric

*To whom correspondence should be addressed. Fax: +49-941-943-4488 (H.Y.). E-mail: hartmut.yersin@chemie.uni-regensburg.de (H.Y.), uwe.monkowius@jku.at (U.V.M.).

(1) Yersin, H., Ed.; *Highly Efficient OLEDs with Phosphorescent Materials*; Wiley-VCH: Weinheim, 2008.
(2) Polikarpov, E.; Thompson, M. E. *Mater. Matters* **2007**, *2*, 21.
(3) Williams, J. A. G.; Develay, S.; Rochester, D. L.; Murphy, L. *Coord. Chem. Rev.* **2008**, *252*, 2596.
(4) Chou, P. T.; Chi, Y. *Chem.—Eur. J.* **2007**, *13*, 380.
(5) Che, C.-M.; Kwok, C.-C.; Lai, S.-W.; Rausch, A. F.; Finkenzeller, W. J.; Zhu, N.; Yersin, H. *Chem.—Eur. J.* **2010**, *16*, 233.
(6) Evans, R. C.; Douglas, P.; Winscom, C. *Coord. Chem. Rev.* **2006**, *250*, 2093.
(7) Holder, E.; Langeveld, B. M. W.; Schubert, U. S. *Adv. Mater.* **2005**, *17*, 1109.
(8) Bolink, H. J.; Coronado, E.; Costa, R. D.; Lardiés, N.; Ortí, E. *Inorg. Chem.* **2008**, *47*, 9149.
(9) Armaroli, N.; Accorsi, G.; Holler, M.; Moudam, O.; Nierengarten, J.-F.; Zhou, Z.; Wegh, R. T.; Welter, R. *Adv. Mater.* **2006**, *18*, 1313.
(10) Rudmann, H.; Shimada, S.; Rubner, M. F. *J. Am. Chem. Soc.* **2002**, *124*, 4918.
(11) Bernhard, S.; Gao, X.; Malliaras, G. G.; Abruña, H. D. *Adv. Mater.* **2002**, *14*, 433.
(12) Slinker, J.; Bernards, D.; Houston, P. L.; Abruña, H. D.; Bernhard, S.; Malliaras, G. G. *Chem. Commun.* **2003**, 2392.
(13) Baldo, M. A.; O'Brien, D. F.; Thompson, M. E.; Forrest, S. R. *Phys Rev. B* **1999**, *60*, 14422.
(14) Yersin, H. *Top. Curr. Chem.* **2004**, *241*, 1.
(15) Hung, L. S.; Chen, C. H. *Mater. Sci. Eng. R* **2002**, *39*, 143.
(16) Yersin, H.; Monkowius, U. International Patents WO2010/00681A1 and DE2008/033563A1
(17) Williams, J. A. G. *Top. Curr. Chem.* **2007**, *281*, 205.
(18) Sajoto, T.; Djurovich, P. I.; Tamayo, A. B.; Oxgaard, J.; Goddard, W. A., III; Thompson, M. E. *J. Am. Chem. Soc.* **2009**, *131*, 9813.
(19) Yang, L.; Okuda, F.; Kobayashi, K.; Nozaki, K.; Tanabe, Y.; Ishii, Y.; Haga, M. A. *Inorg. Chem.* **2008**, *47*, 7154.

Published on Web 07/30/2010

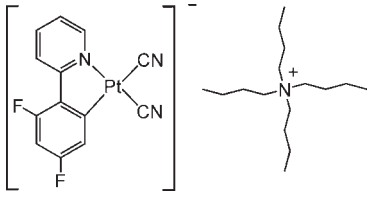

Figure 1. Structure of $[n\text{-}Bu_4N][Pt(4,6\text{-}dFppy)(CN)_2]$.

ligands with high ligand field strengths, such as carbenes.[20] Further, it has been reported that in Pt(II) compounds with terdentate dipyridylbenzene N^C^N ligands, the dd* states are shifted to higher energies when compared to compounds with bidentate phenylpyridine-based N^C ligands because of shorter Pt−C bond lengths in the terdentate complexes.[21−23] Another possibility to shift these quenching states out of reach at ambient temperature is given by the use of strong-field ancillary ligands such as CO and CN^-.[24−26]

In this contribution, we report on the synthesis and crystal structure of $[n\text{-}Bu_4N][Pt(4,6\text{-}dFppy)(CN)_2]$ with 4,6-dFppy = (4′,6′-difluorophenyl)pyridinate and *n*-Bu = *n*-butyl (Figure 1) as well as on detailed photophysical studies of the compound as neat powder and dissolved in tetrahydrofuran (THF), respectively. The applied strategy of attaching electron withdrawing fluorine atoms at the 4- and 6-positions of the phenyl moiety has proven to be successful in stabilizing the highest occupied molecular orbital (HOMO). This leads to a blue-shift of the emission with respect to non-fluorinated compounds.[27−29]

In general, solid state samples of Pt(II) compounds often show photophysical properties which are remarkably different from those of dilute fluid solutions, since the (pseudo) square-planar geometry facilitates interactions of adjacent monomers via Pt-$5d_{z^2}$ and Pt-6s, $6p_z$-overlap or π-stacking effects.[30−34] As a consequence, low-energy emission bands stemming from molecular aggregates[30,31,35] or excimers[21,22,36] occur. However, bulky counterions can suppress such intermolecular interactions in the solid state.[34] In the present case, the bulky $[n\text{-}Bu_4N]^+$ cation prevents close contacts of the $[Pt(4,6\text{-}dFppy)(CN)_2]^-$ anions in the crystal packing. This leads to a close similarity of the emission spectra of the neat powder and of a dilute fluid solution. On the other hand, concerning the emission decay times and the emission quantum yields, distinct differences are observed. The origin of these differences is ascribed to the crystal structure and a stabilization of quenching metal-centered dd* states in solution via molecular distortions and/or bond length elongations. Further insight into the nature of the emitting T_1 state is gained from decay time measurements in frozen THF down to 1.2 K and from a highly resolved low-temperature single-crystal emission spectrum.

2. Experimental Section

Absorption spectra were recorded with a Varian Cary 300 double beam spectrometer. Emission spectra at 300 and at 77 K were measured with a steady-state fluorescence spectrometer (Jobin Yvon Fluorolog 3). Luminescence quantum yields were determined with an integrating sphere (Labsphere, 4P-GPS-033-SL) with highly reflective Spectralon inside coating. The estimated relative error is about ±0.10. Fluid solutions were degassed by at least three pump−freeze−thaw cycles with a final vapor pressure at 77 K of $\approx 10^{-5}$ mbar. Experiments at lower temperatures were carried out in a He cryostat (Cryovac Konti Cryostat IT) in which the He gas flow, He pressure, and heating were controlled. Highly resolved emission spectra were detected with a cooled photomultiplier (RCA C7164R) attached to a triple spectrograph (S&I Trivista TR 555). A pulsed diode laser (PicoQuant PDL 800-B) with a pulse width of about 500 ps and an excitation wavelength of 372 nm or a Nd:YAG laser (IB Laser Inc., DiNY pQ 02) with a pulse width of about 7 ns, using the third harmonic at 355 nm, were applied as excitation sources for decay time measurements. The Nd:YAG laser was also used as excitation source for low-temperature emission spectra. Decay times were registered using a FAST Comtec multichannel scaler PCI card with a time resolution of 250 ps. Elemental analyses were carried out by the Center for Chemical Analysis of the Faculty of Chemistry at the Universität Regensburg. NMR spectra were measured with a Bruker Avance 300 instrument (T = 300 K). Chemical shifts are reported in δ [ppm] relative to external standards (solvent residual peak, 85% H_3PO_4). The NMR spectra were analyzed by first order. Characterization of the signals: s = singlet, d = doublet, t = triplet, q = quartet, m = multiplet, dd = double doublet, dt = double triplet, ddd = double double doublet. Mass spectra were recorded on a Finnigan MAT TSQ 7000 (ESI) instrument.

Materials and Synthesis. K_2PtCl_4, $[n\text{-}Bu_4N]Cl$, KCN, 4,6-difluorophenylboronic acid, 2-bromopyridine, and 2-ethoxyethanol are commercially available and were used without further purification. H-4,6-dFppy is prepared via the Suzuki coupling reactions of 4,6-dFppy boronic acid with 2-bromopyridine. [Pt(4,6-dFppy)(H-4,6-dFppy)Cl] is prepared according to a literature method from H-4,6-dFppy and K_2PtCl_4.[37] $[n\text{-}Bu_4N][Pt(4,6\text{-}dFppy)(CN)_2]$ is synthesized starting from a solution of [Pt(4,6-dFppy)(H-4,6-dFppy)Cl] (100 mg, 0.16 mmol) in CH_2Cl_2 (20 mL) and adding an excess of $[n\text{-}Bu_4N]Cl$ (200 mg, 0.72 mmol) and KCN (50 mg, 0.77 mmol). After 2 h stirring, the solvent is removed under reduced pressure. The residue is washed with water and extracted with CH_2Cl_2. Yellow crystals are obtained by recrystallization from CH_2Cl_2/Et_2O. Yield: 98 mg,

(20) Sajoto, T.; Djurovich, P. I.; Tamayo, A.; Yousufuddin, M.; Bau, R.; Thompson, M. E.; Holmes, R. J.; Forrest, S. R. *Inorg. Chem.* **2005**, *44*, 7992.
(21) Williams, J. A. G.; Beeby, A.; Davies, E. S.; Weinstein, J. A.; Wilson, C. *Inorg. Chem.* **2003**, *42*, 8609.
(22) Farley, S. J.; Rochester, D. L.; Thompson, A. L.; Howard, J. A. K.; Williams, J. A. G. *Inorg. Chem.* **2005**, *44*, 9690.
(23) Rausch, A. F.; Murphy, L.; Williams, J. A. G.; Yersin, H. *Inorg. Chem.* **2009**, *48*, 11407.
(24) Chin, C. S.; Eum, M.-S.; Kim, S. Y.; Kim, C.; Kang, S. K. *Eur. J. Inorg. Chem.* **2007**, 372.
(25) Eum, M.-S.; Chin, C. S.; Kim, S. Y.; Kim, C.; Kang, S. K.; Nam, H. H.; Seo, J. H.; Kim, G. Y.; Kim, Y. K. *Inorg. Chem.* **2008**, *47*, 6289.
(26) Di Censeo, D.; Fantacci, S.; De Angelis, F.; Klein, C.; Evans, N.; Kalyanasundaram, K.; Bolink, H. J.; Grätzel, M.; Nazeeruddin, M. K. *Inorg. Chem.* **2008**, *47*, 980.
(27) Brooks, J.; Babayan, Y.; Lamansky, S.; Djurovich, P. I.; Tsyba, I.; Bau, R.; Thompson, M. E. *Inorg. Chem.* **2002**, *41*, 3055.
(28) Adachi, C.; Kwong, R. C.; Djurovich, P. I.; Adamovich, V.; Baldo, M. A.; Thompson, M. E.; Forrest, S. R. *Appl. Phys. Lett.* **2001**, *79*, 2082.
(29) Yang, X.; Wang, Z.; Madakuni, S.; Li, J.; Jabbour, G. E. *Adv. Mater.* **2008**, *20*, 2405.
(30) Yersin, H.; Gliemann, G.; Rössler, U. *Solid State Commun.* **1977**, *21*, 915.
(31) Gliemann, G.; Yersin, H. *Struct. Bonding* (*Berlin*) **1985**, *62*, 87.
(32) Connick, W. B.; Henling, L. M.; Marsh, R. E.; Gray, H. B. *Inorg. Chem.* **1996**, *35*, 6261.
(33) Lai, S.-W.; Chan, M. C.-W.; Cheung, T.-C.; Peng, S.-M.; Che, C.-M. *Inorg. Chem.* **1999**, *38*, 4046.
(34) Forniés, J.; Fuertes, S.; López, J. A.; Martin, A.; Sicilia, V. *Inorg. Chem.* **2008**, *47*, 7166.
(35) Yersin, H.; Donges, D.; Humbs, W.; Strasser, J.; Sitters, R.; Glasbeek, M. *Inorg. Chem.* **2002**, *41*, 4915.
(36) Pettijohn, C. N.; Jochnowitz, E. B.; Chuong, B.; Nagle, J. K.; Vogler, A. *Coord. Chem. Rev.* **1998**, *171*, 85.
(37) Cho, J.-Y; Suponitsky, K. Y.; Li, J.; Timofeeva, T. V.; Barlow, S.; Marder, S. R. *J. Organomet. Chem.* **2005**, *690*, 4090.

Scheme 1. Synthesis of [*n*-Bu_4N][Pt(4,6-dFppy)$(CN)_2$]

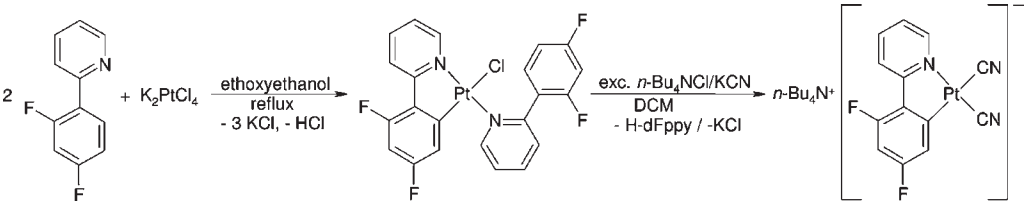

90%. ^{1}H NMR ($CDCl_3$): δ 9.45 (d, J = 4.8, J_{HPt} = 30.1 Hz, 1 H), 8.07 (d, J = 10.0, 1 H), 7.84 (pseudo-t, J = 7.5 Hz, 1 H), 7.71 (dd, J = 2.5, 8.4 Hz, 1 H), 7.11 (pseudo-t, J = 7.0 Hz, 1 H), 6.49 (ddd, J = 2.5, 8.8, 12.9 Hz, 1 H), 3.27−3.33 (m, 8 H), 1.56−1.72 (m, 8 H), 1.41 (q, J = 7.4 Hz, 8 H), 0.94 (t, J = 7.4 Hz, 12 H); ^{13}C{^{1}H} NMR ($CDCl_3$): δ 163.62 (d, J = 7.4 Hz), 161.36 (d, J = 11.0 Hz), 160.92 (dd, J = 2.2, 5.9 Hz), 157.89 (d, J = 11.8 Hz), 152.30, 143.23 (s, CN), 138.21, 128.91, 121.75, 121.43 (d, J = 20.6 Hz), 119.58 (d, J = 14.0 Hz), 115.99 (s, CN), 98.86 (dd, J = 26.9 Hz), 57.76, 23.01, 18.61, 12.63. ^{19}F NMR ($CDCl_3$): δ −108.44 (*pseudo*-quartet, J = 9.0 Hz), −111.30 (*pseudo*-triplet, J = 9.0 Hz); positive ESI-MS: m/z (%) = 242.2 (100) [*n*-Bu_4N]$^+$; negative ESI-MS: m/z (%) = 437.1 (100) [Pt(4,6-dFppy)$(CN)_2$]$^-$; EA ($C_{29}H_{42}N_4F_2Pt$): calc. C 51.24, H 6.23, N 8.24; found C 51.06, H 6.30, N 8.15.

Crystal Structure Determination. Diffraction data for crystals of [*n*-Bu_4N][Pt(4,6-dFppy)$(CN)_2$] were collected with a STOE-IPDS diffractometer[38] with graphite-monochromated Mo-K_α radiation (λ = 0.71073 Å). The structures were solved by direct methods (SIR-97)[39] and refined by full-matrix least-squares on F^2 (SHELXL-97).[40] The H atoms were calculated geometrically, and a riding model was applied during the refinement process.

3. Results and Discussion

3.1. Synthesis and Crystal Structure. The cyclometalated platinum complex [Pt(4,6-dFppy)(H-4,6-dFppy)Cl] (for the crystal structure see the Supporting Information), obtained by the reaction of 4,6-dFppy with K_2PtCl_4, can be used as a convenient starting material for [*n*-Bu_4N]-[Pt(4,6-dFppy)$(CN)_2$]. The latter is prepared as a yellow powder in high yield and purity by the reaction of [Pt(4,6-dFppy)(H-4,6-dFppy)Cl] with an excess of *n*-Bu_4NCl/KCN (Scheme 1). The final product was characterized by NMR spectroscopy, mass spectrometry, and elemental analyses (see Experimental Section). It shows expected ^{1}H- and ^{13}C-NMR signals. The negative ion electrospray mass spectrum is dominated by the peak representing the anion [Pt(4,6-dFppy)$(CN)_2$]$^-$.

Single crystals of [*n*-Bu_4N][Pt(4,6-dFppy)$(CN)_2$] suitable for structure determination by X-ray diffraction are grown by slow gas phase diffusion of Et_2O into a CH_2Cl_2 solution. The material crystallizes in the orthorhombic space group $Pna2_1$ (Z = 4). As depicted in Figure 2, the *n*-Bu_4N^+ cations are squeezed between adjacent platinum complex anions forming alternating layers of cations and anions. Therefore, no π-interactions between the aromatic moieties are present, and adjacent Pt atoms are separated from each other by 8.17 Å. Because of the spatial isolation of the Pt complex anions, no Pt−Pt interactions via orbital overlap are possible. The Pt atoms show a pseudo square-planar coordination geometry with an angular sum of 360.1° (Figure 3). The bite angle of the cyclometalated ligand N1−Pt1−C1 is determined to be 80.6(2)°, and the torsion angle between its aromatic

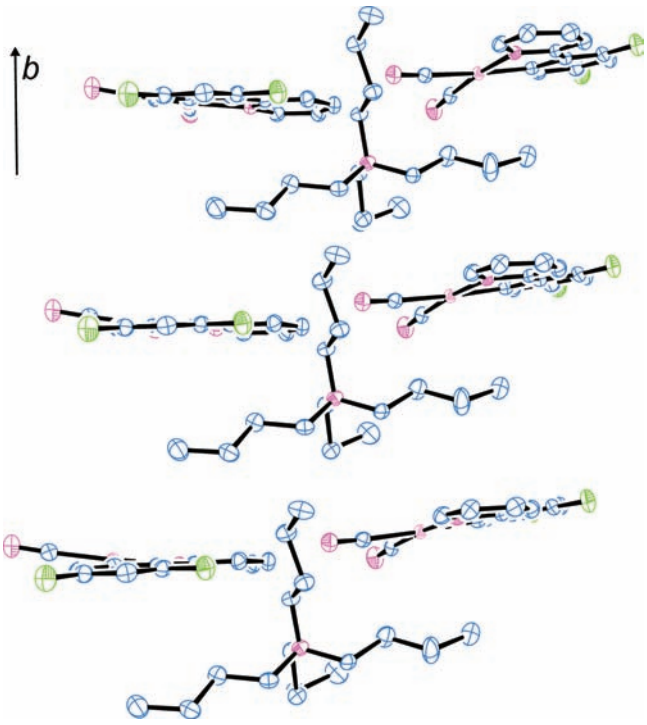

Figure 2. View perpendicular to the *b* axis illustrating the alternation of *n*-Bu_4N^+ cations and complex anions within [*n*-Bu_4N][Pt(4,6-dFppy)-$(CN)_2$] crystals. ORTEP drawing with 50 % probability ellipsoids (H atoms are omitted for clarity). The Pt-Pt separations amount to 8.17 Å.

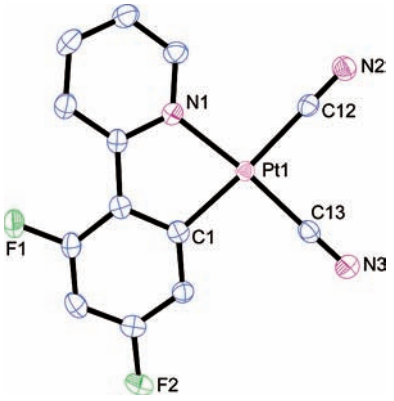

Figure 3. Complex anion in crystals of [*n*-Bu_4N][Pt(4,6-dFppy)$(CN)_2$]. Selected bond lengths [Å] and angles [deg]: Pt1−N1 2.070(3), Pt1−C1 2.032(3), Pt1−C12 2.029(3), Pt1−C13 1.968(3); N1−Pt1−C1 80.6(2), N1−Pt1−C12 95.8(1), C12−Pt1−C13 89.3(1), C1−Pt1−C13 94.4(1).

(38) *Stoe IPDS-software*, version 2.89; Stoe & Cie GmbH: Darmstadt, Germany, 1998.
(39) Altomare, A.; Cascarano, G.; Giacovazzo, C.; Guagliardi, A. *J. Appl. Crystallogr.* **1993**, *26*, 343.
(40) Sheldrick, G. M. *SHELXL-97, Program for crystal structure refinement*; University of Göttingen: Göttingen, Germany, 1997.

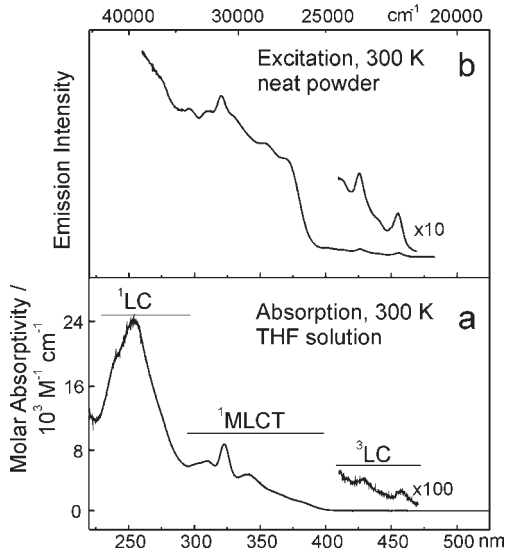

Figure 4. (a) Absorption spectrum of [*n*-Bu_4N][Pt(4,6-dFppy)$(CN)_2$] dissolved in THF ($c \approx 10^{-5}$ mol/L) and (b) excitation spectrum of the neat powder (λ_{em} = 490 nm) at T = 300 K. Note the respective scaling factors.

rings is small [2.7(4)°]. The cyanide ligand cis to the C atom of the aromatic ligand is marginally twisted out of the platinum coordination sphere [N1−Pt1−C13 173.7(1)°] which may result from the small deviation of the phenylpyridine moiety from the ideal coplanar conformation or from packing effects. The cyanide ligand *trans* to the C atom of the cyclometalated ligand features significantly longer bond lengths, reflecting its stronger *trans* effect compared to the nitrogen donor atom [Pt1−C13 1.968(3) vs Pt1−C12 2.029(3) Å]. Conversely, the C≡N bond of the cyanide *trans* to the C atom of the dFppy ligand is slightly shorter than in the other cyanide ligand [C12−N2 1.146(4) vs C13−N3 1.155(4) Å]. These data agree well with those observed for comparable Pt complexes.[34,41−44] Further crystallographic and refinement data can be found in the Supporting Information.

3.2. Photophysical Properties. 3.2.1. Studies at Ambient Temperature and at 77 K. Figure 4 shows the absorption spectrum of [*n*-Bu_4N][Pt(4,6-dFppy)$(CN)_2$] in THF solution ($c \approx 10^{-5}$ mol/L) (a) and an excitation spectrum of the neat powder (b), measured at ambient temperature.

In the energy region above ≈33000 cm^{-1} (300 nm) the absorption spectrum comprises a broad and intense band with a maximum at 39200 cm^{-1} (255 nm, ε = 24600 M^{-1} cm^{-1}) (Figure 4a). In this range, one finds mainly ligand-centered (LC) transitions of the (4,6-dFppy) ligand. The corresponding electronic states are largely of ^{1}LC character. In contrast, the lower lying absorptions down to ≈25000 cm^{-1} (400 nm) cannot be found in the absorption spectrum of the free ligand. This indicates that the corresponding states, which are assigned as singlet states because of the significant extinction coefficients, exhibit strong

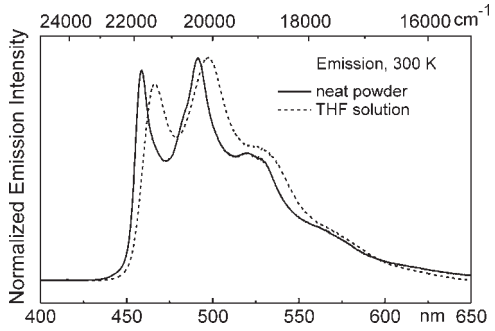

Figure 5. Normalized emission spectra of [*n*-Bu_4N][Pt(4,6-dFppy)-$(CN)_2$] as neat powder (solid line) and dissolved in THF ($c \approx 10^{-5}$ mol/L, dashed line) at T = 300 K, λ_{ex} = 370 nm.

metal-to-ligand charge transfer (MLCT) character. It is remarked that the assignments to LC and MLCT ranges represent only coarse classifications since both types of states can distinctly mix. Two very weak bands ($\varepsilon \approx$ 50 M^{-1} cm^{-1}) at 21850 cm^{-1} (458 nm) and at 23300 cm^{-1} (429 nm) represent largely spin-forbidden transitions from the singlet ground state S_0 to the lowest triplet state T_1, which is mainly of ligand centered character (see below). The peak of lowest energy is assigned to correspond to the electronic origin transition, while the band lying by 1450 cm^{-1} higher in energy corresponds to overlapping vibrational modes of the T_1 state.

In the excitation spectrum of the powder material, depicted in Figure 4b, the low-energy bands governed by the $S_0 \rightarrow T_1$ transition are even more distinct. They are slightly blue-shifted to 22000 cm^{-1} (455 nm) and at 23450 cm^{-1} (426 nm), respectively, compared to the THF solution. The general trend shows that the other bands observed in the excitation spectrum of the powder have counterparts to those found in the absorption spectrum of the solution. As already expected from the crystal structure, this result also indicates that the powder spectrum does not stem from aggregates exhibiting Pt−Pt interactions, since these would lead to pronounced low-energy bands.[35,41,45]

Figure 5 shows the ambient-temperature emission spectra of [*n*-Bu_4N][Pt(4,6-dFppy)$(CN)_2$] in THF solution and as powder material. The emission bands in solution are slightly red-shifted and exhibit slightly larger halfwidths. These effects are typical for polar solvents like THF, which, unlike the situation in the solid powder, allow for dipole relaxation of the solvent molecules when the chromophores are electronically excited.[46] Apart from that, the spectra are very similar. The structured emission at ambient temperature is indicative of an emitting state of largely ligand centered character.[47,48] The bands at 21800 cm^{-1} (459 nm) (neat powder) and at 21450 cm^{-1} (466 nm) (solution), respectively, correspond to the electronic transition between the lowest triplet state T_1 and the singlet ground state S_0. A comparison with the respective low-energy absorption/excitation bands reveals small Stokes shifts of ≈200 cm^{-1} (powder) and ≈450 cm^{-1} (solution), respectively. The larger Stokes shift in solution

(41) Mdleleni, M. M.; Bridgewater, J. S.; Watts, R. J.; Ford, P. C. *Inorg. Chem.* **1995**, *34*, 2334.
(42) Godbert, N.; Pugliese, T.; Aiello, I.; Bellusci, A.; Crispini, A.; Ghedini, M. *Eur. J. Inorg. Chem.* **2007**, 5105.
(43) Yoon, M. S.; Ryu, D.; Kim, J.; Ramesh, R.; Ahn, K. H. *Bull. Korean Chem. Soc.* **2007**, *28*, 2045.
(44) Kvam, P.-I.; Engbretsen, T.; Maartmann-Moe, K.; Songstad, J. *Acta Chem. Scand.* **1996**, *50*, 107.
(45) Ma, B.; Li, J.; Djurovich, P. I.; Yousufuddin, M.; Bau, R.; Thompson, M. E. *J. Am. Chem. Soc.* **2005**, *127*, 28.
(46) Chen, P.; Meyer, T. J. *Chem. Rev.* **1998**, *98*, 1439.
(47) Maestri, M.; Sandrini, D.; Balzani, V.; von Zelewsky, A.; Deuschel-Cornioley, C.; Jolliet, P. *Helv. Chim. Act.* **1988**, *71*, 1053.
(48) Yersin, H.; Donges, D. *Top. Curr. Chem.* **2001**, *214*, 81.

Table 1. Photophysical Data of the Lowest Triplet State of [*n*-Bu_4N][Pt(4,6-dFppy)$(CN)_2$] Dissolved in THF and as Neat Powder

solvent/host	triplet absorption, excitation (300 K) λ_{max}/nm	emission (300 K) λ_{max}/nm	emission (77 K) λ_{max}/nm	ϕ_{PL}/%	τ (300 K)/μs	τ (77 K)/μs
THF	429[a], 458[b]	466[b], 498[a]	460[b], 492[a]	$\ll 1$[c]	0.26[c] (0.19)[d]	21.5
neat powder	426[a], 455[b]	459[b], 491[a]	457[b], 489[a]	60	19.0	17.1

[a] Vibrational satellite band. [b] Electronic origin transition. [c] Deaerated. [d] Air saturated.

is related to a slightly larger geometry rearrangement upon excitation of the complex in the "soft" fluid environment compared to the rigid situation in the powder. The intense vibrational satellite bands at 20350 cm^{-1} (491 nm) (powder) and 20100 cm^{-1} (498 nm) (solution) are separated from the electronic origin band by ≈1450 and ≈1350 cm^{-1}, respectively. These energies are typical for vibrational stretching modes of aromatic ligands.[48−50] Comparable vibrational energies are also found in the absorption/excitation spectra (see above).

The close correspondence of the powder and the fluid solution emission spectra is uncommon for Pt(II) compounds, since in the solid state and also in concentrated solutions and doped polymeric films adjacent monomers frequently interact strongly because of short Pt−Pt separations and/or π-stacking effects. This leads to emission bands which distinctly differ from the monomer emission.[30−36,41] However, the crystal structure of [*n*-Bu_4N][Pt(4,6-dFppy)$(CN)_2$] reveals large Pt−Pt separations of more than 8 Å, which are a consequence of the crystal packing caused by the bulky [*n*-Bu_4N]$^+$ cations (see above). Therefore, strong interactions between adjacent [Pt(4,6-dFppy)$(CN)_2$]$^-$ anions are absent, and the emission results from largely isolated monomers.

Despite the similarity of the emission spectra of the neat powder and of the solution, distinct differences are observed for the emission quantum yields and the emission decay times. The powder sample shows bright sky-blue emission with a remarkably high quantum yield of ϕ_{PL} = 60% and an emission decay time of 19.0 μs. On the other hand, the decay time of a deaerated THF solution amounts to only 260 ns. Despite careful deaeration, the emission quantum yield remains much lower than 1%. Explanations for these huge differences are discussed in section 4.

With temperature reduction to 77 K, the emission spectra of the neat powder and the frozen THF solution are slightly blue-shifted and a little better resolved (not shown). After cooling, the emission decay times are in relatively good correspondence and amount to 17.1 μs (powder) and 21.5 μs (frozen THF), respectively. Photophysical data of [*n*-Bu_4N][Pt(4,6-dFppy)$(CN)_2$] at 300 and 77 K are summarized in Table 1.

3.2.2. Temperature Dependent Emission Decay in THF. Decay time measurements of [*n*-Bu_4N][Pt(4,6-dFppy)$(CN)_2$] in frozen THF down to 1.2 K have been carried out to gain deeper insight into the nature of the emitting triplet state. Such studies are well-known and allow to identify the three substates of the lowest triplet state T_1 and the individual decay times of these substates by

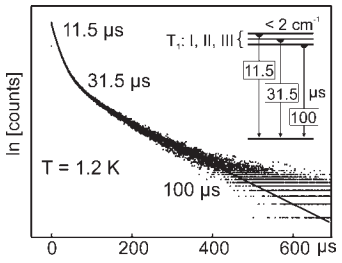

Figure 6. Emission decay of [*n*-Bu_4N][Pt(4,6-dFppy)$(CN)_2$] in frozen THF ($c \approx 10^{-5}$ mol/L, λ_{exc} = 355 nm) at T = 1.2 K. The inset depicts the energy level diagram and the individual decay times of the T_1 substates. The counts measured for t > 400 μs are largely determined by the photomultiplier dark current.

analyzing the temperature-dependent emission decay behavior.[51−53] In particular, the total zero-field splitting energy ΔE(ZFS) represents a useful parameter to classify the emitting state, since it has been shown by an empirical ordering scheme that the magnitude of ΔE(ZFS) displays the effectiveness of SOC to higher lying states and can be correlated with the MLCT contribution in the emitting triplet.[14,48,54,55]

For [*n*-Bu_4N][Pt(4,6-dFppy)$(CN)_2$] in THF, a strongly non-monoexponential decay is observed at 1.2 K, which can be fit by a combination of three exponentials (Figure 6). This indicates that the three T_1 substates are not in a thermal equilibrium at this low temperature. Processes of relaxation (spin−lattice relaxation, SLR), which thermalize the population between the substates, strongly depend on their energy separations and on temperature.[56,57] In the present situation and at T = 1.2 K, these processes are much slower than the individual decay times. Thus, the substates emit independently according to their initial populations with their individual decay times. These are determined to $\tau_I = (100 \pm 10)$ μs, $\tau_{II} = (31.5 \pm 3)$ μs, and $\tau_{III} = (11.5 \pm 2)$ μs. The occurrence of three individual decay times at 1.2 K indicates very small energy separations between the T_1 substates and thus a small total zero-field splitting, presumably being smaller than 2 cm^{-1} (see also below).

With temperature increase, the SLR processes become faster and a thermal equilibrium between the T_1 substates establishes.[57] At 10 K, a monoexponential decay with a time constant of τ_{av} = 23.8 μs is observed. This value decreases only slightly with further temperature increase. At 20 K, for example, the decay constant amounts to 22.7 μs, at 77 K to 21.5 μs, and at 100 K to 21.2 μs. Thus, it can be concluded that no higher lying electronic state is

(49) Amini, A.; Harriman, A.; Mayeux, A. *Phys. Chem. Chem. Phys.* **2004**, *6*, 1157.
(50) Yersin, H.; Humbs, W.; Strasser, J. *Top. Curr. Chem.* **1997**, *191*, 153.
(51) Finkenzeller, W. J.; Yersin, H. *Chem. Phys. Lett.* **2003**, *377*, 299.
(52) Harrigan, R. W.; Crosby, G. A. *J. Chem. Phys.* **1973**, *59*, 3468.
(53) Azumi, T.; O'Donnell, C. M.; McGlynn, S. P. *J. Chem. Phys.* **1966**, *45*, 2735.
(54) Yersin, H.; Finkenzeller, W. J. In *Highly Efficient OLEDs with Phosphorescent Materials*; Yersin, H., Ed.; Wiley-VCH: Weinheim, Germany, 2008; p 1.
(55) Rausch, A. F.; Homeier, H. H. H.; Yersin, H. *Top. Organomet. Chem.* **2010**, *29*, 193.
(56) Scott, P. L.; Jeffries, C. D. *Phys. Rev.* **1962**, *127*, 32.
(57) Yersin, H.; Strasser, J. *Coord. Chem. Rev.* **2000**, *208*, 331.

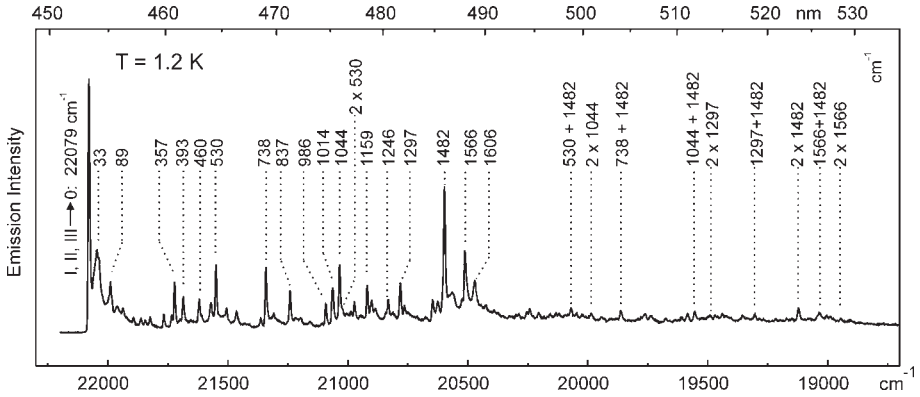

Figure 7. Emission spectrum of a single crystal of $[n\text{-Bu}_4\text{N}][\text{Pt(4,6-dFppy)(CN)}_2]$ (λ_{exc} = 355 nm) at T = 1.2 K. The numbers represent the vibrational energies of the corresponding modes with respect to the electronic 0−0 transition between the T_1 state (with the substates I, II, and III) and the singlet ground state S_0.

thermally populated in this temperature range. If, at a higher temperature, the thermal energy is much larger than the splittings between the T_1 substates [$k_BT \gg \Delta E$-(ZFS)], the thermalized (averaged) emission decay time τ_{av} can be expressed as[58,59]

$$\tau_{av} = 3\left(\frac{1}{\tau_I}+\frac{1}{\tau_{II}}+\frac{1}{\tau_{III}}\right)^{-1} \quad (1)$$

Using the individual decay times as determined at 1.2 K and applying eq 1, one obtains a value of τ_{av} = 23.3 μs, which is in good agreement with the decay time measured at 10 K.

According to the mentioned empirical ordering scheme,[14,48,54,55] the emitting state of $[n\text{-Bu}_4\text{N}][\text{Pt(4,6-dFppy)(CN)}_2]$ with a total zero-field splitting of < 2 cm^{-1} can be assigned to be largely of ligand-centered (^{3}LC, $^3\pi\pi^*$) character with only small MLCT admixtures. This will be further discussed in section 4.

3.2.3. Highly Resolved Emission of a Single Crystal. High-resolution spectroscopy of organo-transition metal compounds in polycrystalline host materials, for example in *n*-alkanes, has proven to be a useful tool to characterize the emitting states (Shpol'skii spectroscopy).[23,35,48,54,55,60] However, since charged molecules are virtually insoluble in *n*-alkanes, only neutral compounds can be investigated in these matrixes. On the other hand, crystalline samples of ionic molecules may also allow to obtain highly resolved emission spectra. If the emitter molecules in the crystal are largely isolated with respect to electronic interactions, the individual chromophores can be spectroscopically investigated.[50,61] In particular, at very low temperature, the chromophores may frequently be regarded as traps in the bulk material and highly resolved spectra can be obtained. Figure 7 shows the emission spectrum of a single crystal of $[n\text{-Bu}_4\text{N}][\text{Pt(4,6-dFppy)(CN)}_2]$ at that temperature.

The most intense line at 22079 cm^{-1} represents the transition of highest energy and is assigned to the electronic 0−0 transition of all three T_1 substates I, II, and III to the singlet ground state S_0. There is no indication that the total zero-field splitting exceeds the upper limit of 2 cm^{-1} as determined for the compound dissolved in THF. At lower energy, a manifold of sharp lines, being less intense than the electronic 0−0 transition, is observed together with a weak inhomogeneous background. Many of these lines correspond to fundamental vibrations. Low energy modes with energies up to ≈100 cm^{-1} relative to the electronic 0−0 transitions are largely determined by vibrations of the compound in its matrix cage, that is, of the chromophore traps. These satellites represent so-called local phonon modes, for example, the 33 and 89 cm^{-1} lines. It should be noted that interactions of low energy vibrations of the compound with such cage modes manifest themselves at least up to ≈150 cm^{-1}.[62] Overlapping with this energy range up to ≈600 cm^{-1}, metal−ligand (M-L) vibrational satellites can be found, for example, at 357 and 530 cm^{-1}, while fundamentals with energies higher than ≈600 cm^{-1} can usually be assigned as internal ligand modes, for example 1044, 1297, 1482, and 1566 cm^{-1}.[48,50] For these intense fundamental modes, one can observe weak second members of progressions and also combinations. From the occurrence of progressions it is concluded that the corresponding modes represent totally symmetric Franck−Condon (FC) active modes. The assignment of these modes as being Franck−Condon induced is supported by a comparison of their vibrational energies with those of FC active modes which were observed in the highly resolved emission spectra of Pt(4,6-dFppy)(acac) (acac = acetylacetonate) in *n*-octane.[55,63] The corresponding energies are compared in Table 2. Most modes can be well correlated. In cases in which the vibrational energies show differences of more than 5 cm^{-1}, the given correlations are substantiated by the observed intensity patterns in the respective emission spectra. Almost all correlated vibrations of $[\text{Pt(4,6-dFppy)(CN)}_2]^-$ have lower energies than those of Pt(4,6-dFppy)(acac). This behavior might be related to the different charges of the complexes. Presumably, the distinct reduction of force constants, as observed for $[\text{Pt(4,6-dFppy)(CN)}_2]^-$, is induced by the negative charge, which may be distributed at least in part

(58) Tinti, D. S.; El-Sayed, M. A. *J. Chem. Phys.* **1971**, *54*, 2529.
(59) Finkenzeller, W. J.; Stössel, P.; Yersin, H. *Chem. Phys. Lett.* **2004**, *397*, 289.
(60) Rausch, A. F.; Yersin, H. *Chem. Phys. Lett.* **2010**, *484*, 261.
(61) Yersin, H.; Kratzer, C. *Coord. Chem. Rev.* **2002**, *229*, 75.
(62) Becker, D.; Yersin, H.; von Zelewsky, A. *Chem. Phys. Lett.* **1995**, *235*, 490.
(63) Rausch, A. F.; Thompson, M. E.; Yersin, H. *Chem. Phys. Lett.* **2009**, *468*, 46.

Table 2. Comparison of the Energies of Franck-Condon Active Vibrational Modes in the Emission of Single-Crystal [*n*-Bu_4N][Pt(4,6-dFppy)$(CN)_2$] Measured at 1.2 K and of Pt(4,6-dFppy)(acac) in *n*-Octane Measured at 20 K (Taken from ref 55)

[*n*-Bu_4N][Pt(4,6-dFppy)$(CN)_2$]/cm^{-1}	Pt(4,6-dFppy)(acac)/cm^{-1}
357	371
530	530
738	743
837	858
986	990
1014	1022
1044	1056
1159	1171
1246	1261
1297	1310
1482	1497
1566	1570
1606	1620

also over antibonding π^* ligand orbitals. A related situation has been reported for the vibrational ligand modes of $[Ru(bpy)_3]^{2+}$ as compared to those of $Li^+(bpy)^-$ (with bpy = 2,2′-bipyridine).[64] Also in this case, all vibrational modes of the reported range of $(bpy)^-$ have lower energies than those of bpy.

For many compounds, the emission of substate I differs distinctly from the emissions of the higher lying substates II and III. This is a consequence of the frequently much lower transition probability of the electronic 0−0 transition I ↔ 0 as compared to the transitions II ↔ 0 and III ↔ 0.[23,48,54,55,63] Thus, the emission spectra stemming from substate I frequently do not show FC activity. Instead, the radiative decay is facilitated by processes of spin-vibronic coupling (often referred as Herzberg−Teller coupling, HT) of substate I to higher lying singlet states.[48,50,54,65] These processes induce intensity to (mostly) non-totally symmetric vibrational modes, preferably in the M-L range, but not to the corresponding electronic 0−0 transition.[48] In the present case, the modes with energies of 393 and 460 cm^{-1} might represent such HT active vibrations, since HT modes with similar energies occur in the emission of substate I of Pt(4,6-dFppy)(acac) in *n*-octane.[55] A deeper assignment is not in the scope of this investigation.

4. Assignments and Conclusions

[*n*-Bu_4N][Pt(4,6-dFppy)$(CN)_2$] exhibits sky-blue monomer phosphorescence both as neat powder and in dilute THF solution. However, at ambient temperature, the emission decay times and the phosphorescence quantum yields are remarkably different. For the powder material, a high emission quantum yield of ϕ_{PL} = 60% is observed, and the emission decay time of 19.0 μs at 300 K does not deviate strongly from the value of 17.1 μs obtained at 77 K. On the other hand, in deaerated ambient temperature solution, the compound is only weakly emissive ($\phi_{PL} \ll 1\%$) and the decay time of 260 ns is much shorter than the value of 21.5 μs obtained for a frozen solution at 77 K. This behavior was also observed for other blue-emitting Pt(II) compounds containing the (4,6-dFppy)-ligand and was assigned to the thermal population of a higher lying metal-centered electronic state of mainly dd* character.[27,55] It is well established that such states, which are characterized by strongly distorted geometries with respect to the electronic ground state, exhibit a high non-radiative deactivation rate and thus can quench the emission.[17−19] For [*n*-Bu_4N][Pt(4,6-dFppy)$(CN)_2$] as neat powder, the lowest dd* states seem to have an energy separation from the emitting triplet state T_1 of at least 3000 cm^{-1}, since no significant emission quenching is observed at ambient temperature. On the other hand, a distinct energy stabilization of the dd* states can lead to an effective quenching of the emission in solution. It is not straightforward to predict the reason for this energy stabilization, but we assume that the compound can undergo a geometry change upon electronic excitation in the "soft" fluid solution. Most likely, elongations of Pt−N and Pt−C bonds as well as slight tetrahedral distortions may be involved. These effects lead to a decrease of the ligand field strength and thus to a stabilization of quenching dd* states. As neat powder or as frozen solution, these distortions are largely suppressed by the rigid surroundings. Similar models have been applied to explain the relatively high emission quantum yields of Ru(II) polypyridine compounds in rigid host media like zeolites,[66] oxalate networks,[67] glasses,[68] or polymeric matrixes[69] when compared to fluid solutions. It is stressed that we cannot completely rule out exciplex formation with solvent molecules as relevant quenching mechanism in solution, as often observed for cationic Pt(II) compounds[70] and recently also reported for a phenylpyridine based neutral Pt(II) emitter.[71] In the latter case, the strong tendency to undergo exciplex quenching in polar solvents was related to a moderate reduction potential (−1.43 V vs Fc/Fc^+) and thus a high nucleophilicity of the compound. Electrochemical data are not yet available for [Pt(4,6-dFppy)$(CN)_2]^-$, but the related compounds Pt(4,6-dFppy)(acac) and [Pt(ppy)$(CN)_2]^-$ (ppy^- = phenylpyridinate) exhibit much more negative potentials of −2.29[27] and −2.36 V[72] (vs Fc/Fc^+), respectively. Thus, it is unlikely that the negatively charged [Pt(4,6-dFppy)$(CN)_2]^-$ forms exciplexes with THF solvent molecules.

From investigations of many organo-transition metal compounds, an empirical ordering scheme has been derived which shows that the magnitude of zero-field splitting energy ΔE(ZFS) of the T_1 state into substates is related to the amount of its MLCT (metal-to-ligand charge transfer) character.[48,54,55,57] A significant amount of ΔE(ZFS) can only result if SOC between the different T_1 substates and higher lying singlet and triplet states of MLCT character is effective.[54,55] For [*n*-Bu_4N][Pt(4,6-dFppy)$(CN)_2$], the emitting triplet state exhibits a very small ZFS of $< 2\ cm^{-1}$. Thus, the T_1 state can be classified to be largely of ligand centered (^{3}LC, $^3\pi\pi^*$) character. Furthermore, since for these states SOC to higher lying ^{1}MLCT states is weak, relatively small radiative decay rates for the transitions of the T_1 substates to

(64) Bradley, P. G.; Kress, N.; Hornberger, B. A.; Dallinger, R. F.; Woodruff, W. H. *J. Am. Chem. Soc.* **1981**, *103*, 7441.
(65) Denning, R. G. In *Vibronic Processes in Inorganic Chemistry*; Flint, C. D., Ed.; Kluwer: Dordrecht, The Netherlands, 1989.
(66) Maruszewski, K.; Strommen., D. P.; Kincaid, J. R. *J. Am. Chem. Soc.* **1993**, *115*, 8345.
(67) von Arx, M. E.; Burattini, E.; Hauser, A.; van Pieterson, L.; Pelleaux, R.; Decurtins, S. *J. Phys. Chem. A* **2000**, *104*, 883.
(68) Danielsson, E.; Lumpkin, R. S.; Meyer, T. J. *J. Phys. Chem.* **1987**, *91*, 1305.
(69) Thompson, D. W.; Fleming, C. N.; Myron, B. D.; Meyer, T. J. *J. Phys. Chem. B* **2007**, *111*, 6930.
(70) McMillin, D. R.; Moore, J. J. *Coord. Chem. Rev.* **2002**, *229*, 113.
(71) Perez, M. D.; Djurovich, P. I.; Hassan, A.; Cheng, G. Y.; Stewart, T. J.; Aznavour, K.; Bau, R.; Thompson, M. E. *Chem. Commun.* **2009**, 4215.
(72) Kvam, P.-I.; Puzyk, M. V.; Cotlyr, V. S.; Balashev, K. P.; Songstad, J. *Acta Chem. Scand.* **1995**, *49*, 645.

the singlet ground state are expected. Indeed, with ϕ_{PL} = 60% and $\tau = 19.0\ \mu s$, the averaged radiative decay rate[73] of the three substates amounts to $k_r = 3.2 \times 10^4\ s^{-1}$ for a neat powder sample at 300 K. For Ir(III) complexes representing typical MLCT emitters, such as $Ir(ppy)_3$[18,51,74] or the heteroleptic compounds $Ir(4,6\text{-}dFppy)_2(acac)$[75] and $Ir(4,6\text{-}dFppy)_2(pic)$[76] (pic = picolinate), the averaged radiative decay rates are at least one order of magnitude larger. The high emission quantum yield of neat [*n*-Bu_4N][Pt(4,6-dFppy)$(CN)_2$] is only possible because of the low averaged non-radiative decay rate[73] of $k_{nr} = 2.1 \times 10^4\ s^{-1}$, which is a consequence of the facts that (i) quenching metal centered dd* states are thermally not accessible at ambient temperature (see above) and (ii) non-radiative deactivation according to the energy gap law is ineffective because of the large energy gap between T_1 and S_0 of about 22000 cm^{-1}.[18,77,78]

For completeness, it is mentioned that the high emission quantum yield of $\phi_{PL} = 60\%$ of neat [*n*-Bu_4N][Pt(4,6-dFppy)$(CN)_2$] might suggest a good electroluminescence performance. On the other hand, the emission decay time of 19 μs is relatively long. Thus, saturation and triplet−triplet annihilation effects might lead to an efficiency decrease (roll-off) at higher current densities or in high brightness applications.[79,80] However, the use of this material in solid state electroluminescent devices in which only small current densities are needed seem to be suitable.

In conclusion, blue light emitters are very sensitive with respect to quenching processes via higher lying dd* states. In particular, slight geometry changes of the emitting triplet state relative to the electronic ground state may lead to an energetic stabilization of these states and to efficient quenching. However, rigid environments can effectively prevent these effects, and bright ambient temperature phosphorescence can result even in the case of relatively low radiative decay rates.

Acknowledgment. We thank the *Bundesministerium für Bildung and Forschung* (*BMBF*) for the funding of our research.

Supporting Information Available: Crystal structures of [Pt(4,6-dFppy)(H-4,6-dFppy)Cl], crystal data, data collection, and structure refinement parameters for [Pt(4,6-dFppy)(H-4,6-dFppy)Cl] and [*n*-Bu_4N][Pt(4,6-dFppy)$(CN)_2$. X-ray crystallographic data for [Pt(4,6-dFppy)(H-4,6-dFppy)Cl] and [*n*-Bu_4N][Pt(4,6-dFppy)$(CN)_2$ in CIF format. This material is available free of charge via the Internet at http://pubs.acs.org.

(73) Radiative and non-radiative decay rates were calculated according to the equation $\phi_{PL} = k_r\tau = k_r/(k_r + k_{nr})$.

(74) Hofbeck, T.; Yersin, H. *Inorg. Chem.*, accepted for publication.
(75) Rausch, A. F.; Thompson, M. E.; Yersin, H. *J. Phys. Chem. A.* **2009**, *113*, 5927.
(76) Rausch, A. F.; Thompson, M. E.; Yersin, H. *Inorg. Chem.* **2009**, *48*, 1928.
(77) Kober, E. M.; Caspar, J. V.; Lumpkin, R. S.; Meyer, T. J. *J. Phys. Chem.* **1986**, *90*, 3722.
(78) Stufkens, D. J.; Vlček, A., Jr. *Coord. Chem. Rev.* **1998**, *177*, 127.
(79) Giebink, N. C.; Forrest, S. R. *Phys. Rev. B* **2008**, *77*, 235215.
(80) Staroske, W.; Pfeiffer, M.; Leo, K.; Hoffmann, M. *Phys. Rev. Lett.* **2007**, *98*, 197402.